

文章编号: 0258-7025(2009)12-3299-09

Review of Laser Assisted Machining of Ceramics

(Invited Paper)

S. Sun^{1,3} M. Brandt^{1,3} M. S. Dargusch^{2,3,4}

¹Industrial Laser Applications Laboratory, IRIS, Faculty of Engineering and Industrial Sciences,
Swinburne University of Technology, Hawthorn, Victoria, Australia
²School of Engineering, University of Queensland, Queensland, Australia
³CAST Cooperative Research Centre, Australia
⁴Defence Materials Technology Centre, Australia

Corresponding author: ssun@groupwise.swin.edu.au

Received October 13, 2009

Abstract Laser assisted machining (LAM) takes the advantages of local heating and softening of workpiece by laser beam in front of the cutting tool. The local softening of workpiece at the shear zone enables much easier plastic deformation during machining. This paper reviews the up-to-date progress on LAM of ceramics. It covers the laser beam integration with cutting tools, analysis of temperature distribution around the cutting region, material removal mechanism, tool wear mechanism, and optimization of LAM. The benefit of LAM and its optimization are discussed in terms of material removal temperature.

Key words laser technique; laser assisted machining; thermally enhanced machining; material removal temperature

CLCN: TG485

Document Code: A

doi: 10.3788/CJL20093612.3299

1 Introduction

The demand for higher strength and heat resistant materials is increasing, particularly in industry for aerospace applications. However these materials are often difficult to machine due to their physical and mechanical properties such as high strength and low thermal conductivity, which make the cutting forces and cutting temperature higher and lead to a shorter tool life. Because the flow stress and strain hardening rate of materials normally decrease with increasing temperature due to the thermal softening (as shown in Fig. 1), the thermally enhanced machining becomes possible while machining hard-to-machine materials^[1].

Thermally enhanced machining (TEM) is a

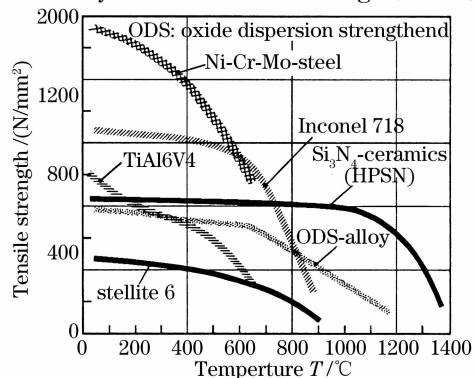


Fig. 1 Effect of temperature on ultimate tensile strength for various materials^[1]

process that uses an external heat source, such as plasma^[2~5], laser beam, gas flame^[6~8], and induction^[9] to heat the workpiece locally in front of the cutting tool during machining (Fig. 2), which changes the material's behaviour from brittle to ductile and therefore allows difficult-to-machine materials to be machined with greater ease^[10]. Therefore, the material removal rate and productivity can increase. This paper reviews the TEM process of ceramics. The review concentrates on laser assisted machining (LAM), because of the advantage of laser beam over other heat sources, such as its rapid and local heating due to its controllable spot size and intensive power density, which leads to a small heat-affected zone and lower thermal distortion.

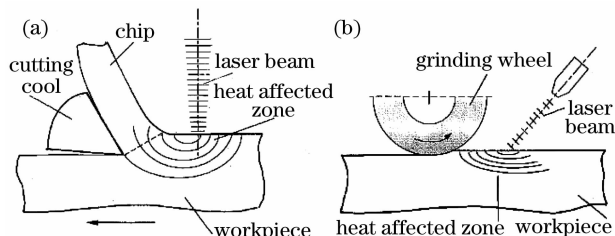


Fig. 2 Illustration of LAM in (a) turning and (b) grinding operations^[10]

2 Integration of a Laser Beam with Machining Applications

The laser beam is positioned in such a way as

to achieve a uniform temperature distribution at the cutting edge without heating the cutting tool. This position depends on the machining operations.

2.1 Turning

For the turning operation, it is relatively simple to integrate a laser beam with the lathe due to the stationary nature of the cutting tool. The laser beam variables are its position, spot size, incident angle, and tool-beam distance. In most of the reported works on laser assisted turning, the laser beam is normal to the workpiece surface^[11~16], as shown in Fig. 3. The advantage of this arrangement is that the machining is easy and does not result in heating of the machined surface, but the large temperature gradient through thickness exists at the cutting edge and the temperature might not be high enough for a deep cut. Furthermore, the exposing of cutting tool surface to the high surface temperature may be detrimental for cutting a workpiece material which has a high chemical reactivity with the cutting tool.

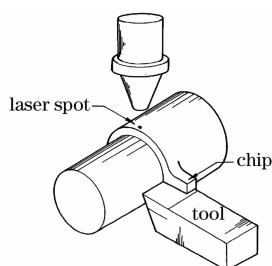


Fig. 3 Setup LAM with laser beam normal to workpiece surface^[15]

Alternatively, the laser beam can be incident on the chamfer surface^[17~19] (as shown in Fig. 4). Higher and uniform reduction of cutting forces in the three directions is achieved^[17,18,20,21]. With an appropriate control of the beam position on the chamfer surface, there is no change in microstructure from the heat remaining in the vicinity of the machined surface and the tool does not directly contact with the laser heated workpiece surface. Shin *et al.*^[22~24] used multiple distributed laser units simultaneously heating both the workpiece and chamfer surface to create the desired temperature distribution through the depth of cut in the workpiece which resulted in the longer tool life (Fig. 5). The laser spot size is required to cover the chamfer surface to achieve uniform reduction of cutting forces in the x , y , and z directions^[17], however, even partial coverage of the chamfer surface by the laser beam close to the machined surface can dra-

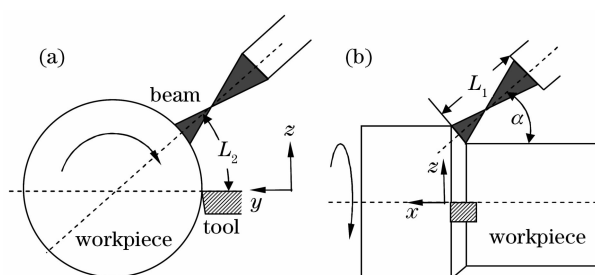


Fig. 4 Relative position of laser beam, workpiece, and cutting tool in laser assisted turning operation. (a) end-view; (b) side-view^[17]

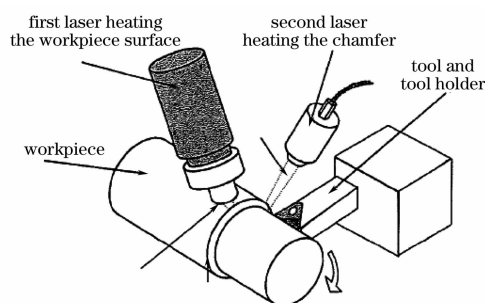


Fig. 5 Laser assisted turning utilizing two laser units^[22] automatically reduce the tool wear^[18].

The position of the laser beam relative to the tool is critical. Tool-beam distance together with cutting speed determines the time interval between the laser heating and cutting operation and therefore the temperature distribution at the cutting zone. It is found that the larger reduction in the cutting force is achieved with the laser spot positioned closer to the cutting tool when cutting hardened steel^[21], commercially pure titanium^[17], and high chromium white cast iron^[25]. However, if the tool-beam distance is too short, the tool may be damaged by over heating, the chips may fly into the laser beam, become molten, and drop onto the machined surface^[26]. Therefore, the tool must be kept at a minimum distance from the laser beam.

2.2 Milling

Integration of the laser beam while milling with the rotating tool is a complicated task. Generally, the beam can be arranged separately to the tool or integrated with the spindle.

For surface milling, the easiest way is to set the beam in front of the tool in the feed direction as shown in Fig. 6. The limited spot size of the external heat source limits the ability to cover the width of cut by a single spot in most applications. Therefore, the beam can only heat part of the cut width. This could be the middle (position 1)^[27] or tool entry point (position 2) or both entry and exit points

(position 2 plus position 3) by two beams^[4,28]. A high power laser, multiple beams or line beam are required to cover the width of the cutting zone (position 4)^[1,28–30].

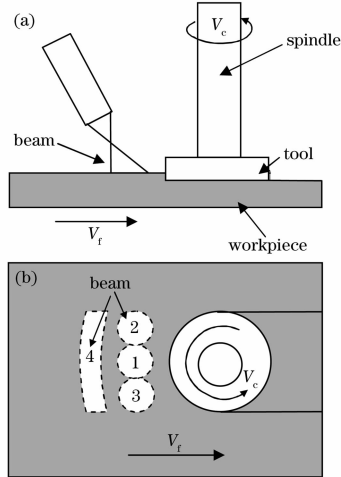


Fig. 6 Illustration of integration of beam with cutting tool for surface milling. (a) side view; (b) top view

Since the dynamic impact on the cutting tool as the rotating tool intermittently engaging with workpiece at the entry point causes significant vibration and ultimately tool fracture, laser beam heating at the entry point is more significant for longer tool life and reduction of chatter. If the beam is moved by additional motors, flexibility can be achieved by aligning the beam with the feed direction of the cutting tool^[29] or by scanning the beam to cover the width of cutting zone.

Instead of heating the top surface of workpiece with a separated beam, two concepts were proposed to integrate the beam with the machine tool^[31,32], and these were proposed for the in-situ laser materials processing (hardening, marking, etc.) during machining. The integration of laser beam with machining tool can be achieved by 1) coupling the beam in the front of the spindle by an interface radial to the tool axis; 2) the laser beam is delivered axially through the spindle and the end beam tool can be rotated with the spindle as shown in Fig. 7.

2.3 Other Processing Processes

Laser preheating has been successfully integrated with planning of Al_2O_3 ^[33], burnishing of steels (as shown in Fig. 8^[34]), dressing^[35–37], grinding^[38], and drilling^[39] in which the laser beam locally heats the workpiece before the planning, burnishing, and dressing tools and through centre-hollow drill tool.

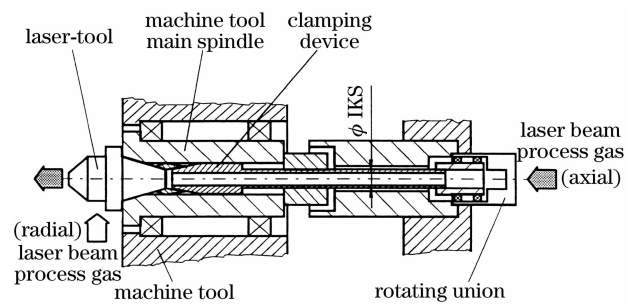


Fig. 7 Concept of radial and axial beam delivery in a milling machine^[31]

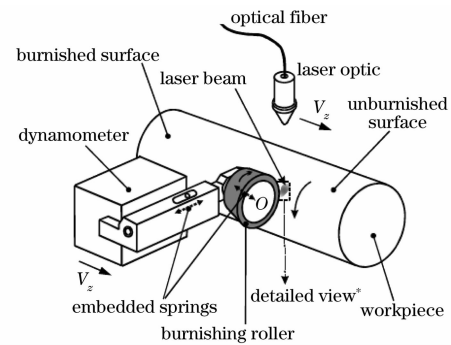


Fig. 8 Setup for laser assisted burnishing^[34]

3 Temperature Distribution Due to Laser Radiation

The operating conditions of LAM need to be controlled within an optimal range for each given workpiece material to achieve good machining results in terms of longer tool life and better surface integrity^[40]. It is found that the temperature is the predominant variable affecting LAM process, as a too high temperature may prematurely degrade the cutting tool and cause workpiece subsurface damage, while a too low temperature will not realize the maximum benefit of the LAM^[23].

The material removal temperature, T_{mr} , which is defined as the average temperature of material as it enters the shear deformation zone^[27], plays a key role in the LAM process. This needs to be controlled to achieve the full benefits of LAM without melting the workpiece or leaving undesirable microstructure alteration in the machined workpiece. Because the deformation behaviour of workpiece material is strongly dependent on the temperature, it is therefore essential to know the temperature distribution from the surface through the thickness up to the cutting edge and optimize it in accordance with the machining parameters. The surface temperature of workpiece subjected to laser radiation can be measured by high speed, high-spatial resolution pyrometers^[11,41–44] and infrared camer-

as^[24,30,45-47]. The optimum surface heating temperature by the laser can be determined by the tool wear resistance and is about 1600~1800 K for Mo and 1550 ± 25 K for W^[41].

A transient, three-dimensional heat transfer model of the thermal response of rotating opaque cylindrical workpiece (silicon nitride, Si₃N₄) subjected to laser radiation with and without the material removal process has been developed by Rozzi *et al.*^[11,48-50]. The governing equation for a transient heat transfer in a rotating cylinder in a cylindrical coordinate system is written as

$$\frac{1}{r} \frac{\partial}{\partial r} \left(kr \frac{\partial T}{\partial r} \right) + \frac{1}{r^2} \frac{\partial}{\partial \varphi} \left(k \frac{\partial T}{\partial \varphi} \right) + \frac{\partial}{\partial z} \left(k \frac{\partial T}{\partial z} \right) + q''' = \rho c_p \omega \frac{\partial T}{\partial \varphi} + \rho c_p V_z \frac{\partial T}{\partial z} + \rho c_p \frac{\partial T}{\partial t}, \quad (1)$$

where k is the thermal conductivity, ρ is the density, c_p is the specific heat, ω is the workpiece rotational speed, and q''' is the volumetric heat generation, which is calculated as

$$\begin{cases} q''' = 0, & \text{without material removal} \\ q''' = \frac{0.85(F_c \bar{V}_w - F_{ct} V_{chip})}{(dL_f/10)} & \text{with material removal} \end{cases}, \quad (2)$$

where F_c is the main cutting force, \bar{V}_w is the average workpiece velocity perpendicular to the cutting tool over the depth of cut, F_{ct} is the friction force, V_{chip} is the average chip velocity on the tool rake face, d is the depth of cut, and L_f is the tool feed.

The external heating of the workpiece leads to high temperature at the shear zone, which results in a reduction in the shear flow stress of the workpiece. Therefore, the heat generation due to the plastic deformation in shear zone is reduced compa-

ring with the conventional machining process^[14].

By setting appropriate boundary conditions at workpiece surface, centreline of the workpiece, end faces of workpiece, in circumferential direction, material removal plane, and initial temperature^[11,49], the temperature field can be calculated.

The model analyses were validated by comparing the predicted surface temperature histories with the measured temperature using pyrometers and infrared cameras over a wide range of operating conditions with and without material removal process^[11,49], and by comparing the depth of heat-affected zone for some alloys^[51]. The validated thermal model reveals the temperature distribution on the surface and through thickness (Figs. 9 and 10). It shows large temperature gradient in all three coordinate directions. With the beam incident on the workpiece surface, temperature gradient exists through the depth of cut and becomes larger with the greater depth of cut at the cutting plane.

This model was modified and applied to laser assisted turning of cylindrical workpiece of semi-transparent ceramics^[12], mullite^[44], Si₃N₄ with complex machined feature^[47], Inconel 718 alloy^[24], austenite stainless steel^[23], and laser assisted milling of Inconel 718 alloy and Si₃N₄^[30].

The material removal temperature (T_{mr}) is critical for LAM process. The optimum of LAM operations (longer tool life, better surface integrity and damage-free part) can be ensured when T_{mr} is maintained in a proper range, which is between 1270 and 1490 °C for Si₃N₄^[52], 900 and 1100 °C for partially-stabilized zirconia (PSZ)^[53], and 1043 and 1215 °C for mullite^[44,54], respectively. The model

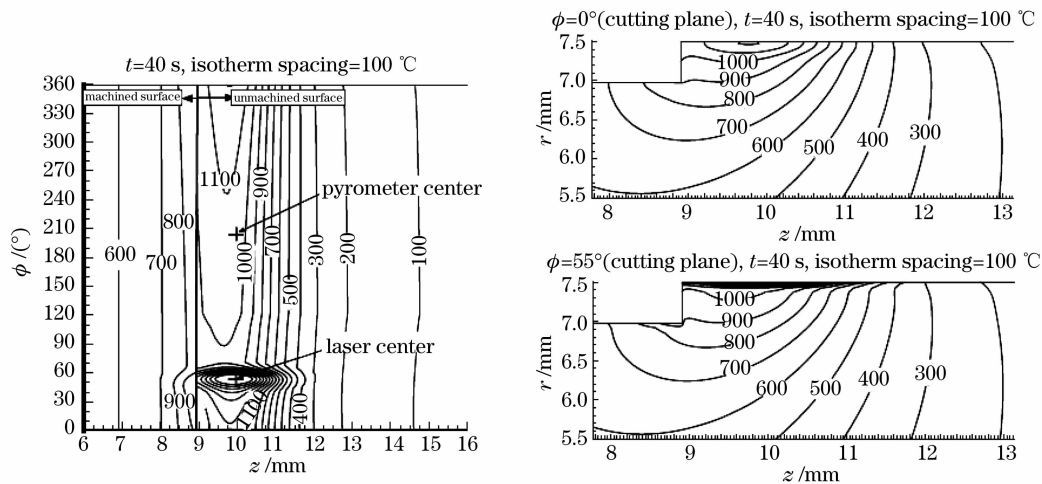


Fig. 9 Predicted temperature on the surface and through thickness at cutting plane ($\phi = 0^\circ$) and laser center ($\phi = 55^\circ$) for LAM of partially-stabilized zirconia^[12]

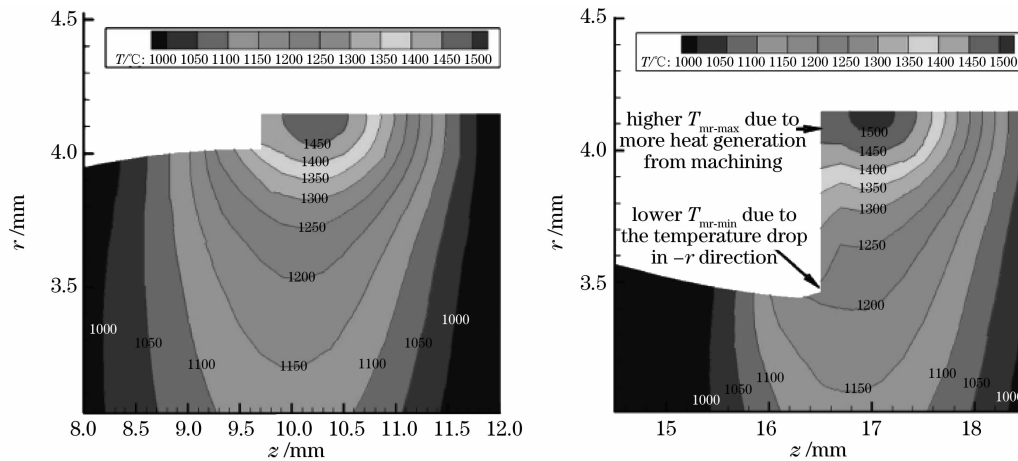


Fig. 10 Temperature distribution through thickness for various depths of cut during LAM of Si_3N_4 [47]

analysis can optimize the cutting conditions to ensure that the material removal temperature is within these ranges.

Since the laser preheating increases the temperature of workpiece before cutting, phase transformation may occur in the heated area. This area is detrimental if it remains after cutting for some alloys, for example the fatigue life is sensitive to the hardness and microstructure in the subsurface such for some workpiece materials as the Ti6Al4V alloy [4]. The model analysis can predict the thickness of the phase transformation layer and select the laser power to ensure that the phase transformation layer can be machined off [51,55,56]. Because the material removal temperature decreases with cutting speed due to the decreasing beam-workpiece interaction time, therefore, the benefit of LAM, such as force reduction and longer tool life, reduces with increasing cutting speed [14,17,21].

4 Machining of Ceramics with the Assistance of a Laser Beam

Advanced engineering ceramics are increasingly used in automotive, aerospace, military, medical, and other applications due to their high temperature strength, low density, thermal and chemical

stability, and good wear resistance. Ceramics are difficult to machine using conventional techniques because of their hardness and brittleness [57]. Machining of these ceramics is a high cost process because of the short tool life, which often results in surface cracking and subsurface damage.

4.1 Material Removal Mechanisms and Chip Formation

The strength of ceramics, such as Si_3N_4 , reduces at high temperature (as shown in Fig. 1) due to the softening of a glassy phase at the grain boundaries. When the cutting tool is engaged with the laser heated workpiece, the material can be removed mainly due to the combination of brittle fracture and plastic deformation [33,52~54,58]. The material removed with LAM of Si_3N_4 is due to 1) plastic deformation in the shear zone which is characterized by viscous flow of a glassy grain boundary phase material and reorientation of the $\beta\text{-Si}_3\text{N}_4$ grains and 2) segmentation of chips as results of the initiation, coalescence, and propagation of intergranular microcracks [52,58].

There are three types of chip formed during LAM of Si_3N_4 and mullite as shown in Fig. 11. It is found that the average near-chamfer surface temperature ($T_{s, \text{ch}}$) [59] or average material removal temperature ($T_{\text{mr}, \text{se}}$) and ratio of feed force to main

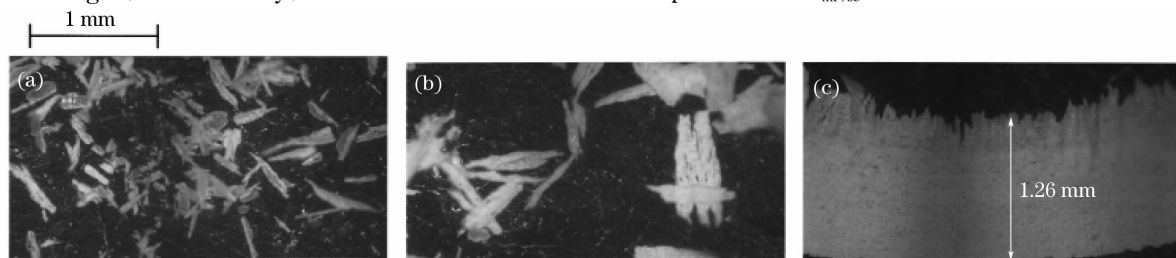


Fig. 11 Morphology of chips formed during LAM of Si_3N_4 . (a) fragmented; (b) semi-continuous; (c) continuous [59]

Table 1 Chip morphology, formation mechanisms, and formation conditions for LAM of Si_3N_4 ^[59] and mullite^[54]

Morphology	Formation mechanisms	Conditions	
		Si_3N_4	Mullite
Fragmented	Brittle fracture	$T_{s, \text{ch}} < 1151 \text{ }^\circ\text{C}$	$F_t/F_c > 1, 800 \text{ }^\circ\text{C} < T_{\text{mr, se}} < 1000 \text{ }^\circ\text{C}$
Semi-continuous	Local brittle fracture and plastic deformation	$1151 \text{ }^\circ\text{C} < T_{s, \text{ch}} < 1305 \text{ }^\circ\text{C}$	$F_t/F_c < 1, 1000 \text{ }^\circ\text{C} < T_{\text{mr, se}} < 1300 \text{ }^\circ\text{C}$
Continuous	Plastic deformation	$T_{s, \text{ch}} > 1329 \text{ }^\circ\text{C}$	$F_t/F_c < 1, T_{\text{mr, se}} > 1300 \text{ }^\circ\text{C}$

cutting force (F_t/F_c)^[54] plays a key role in the chip formation for Si_3N_4 and mullite as listed in Table 1. The mechanisms have been confirmed by FEM analysis^[60].

Despite that there is no continuous and semi-continuous chip formed with LAM of PSZ, plastic deformation occurs during chip formation in addition to brittle fracture^[53]. The plastic deformation results from high temperature dislocation motion and dynamic recrystallization that leads to smaller grain size and preferred grain orientation in the LAM surface^[53,61].

4.2 Cutting Forces and Specific Cutting Energy

The cutting zone stress decreases with increasing material removal temperature and feed but is not significantly dependent on the cutting speed during LAM^[58]. All three components of cutting force are independent of cutting time (or tool wear), which is due to the formation of thin glassy workpiece material which acts as a lubricant on the wear land^[58].

The cutting forces and specific cutting energy decrease with increasing laser power or surface temperature while cutting ceramics such as mullite^[54], magnesia-partially-stabilized zirconia (PSZ)^[53], and Si_3N_4 ^[27,52,59,62] because of the increasing material removal temperature with laser power, but are not significantly affected by the laser-tool lead distance L_1 [59]. Not only the cutting forces, but the ratios of the thrust force, feed force, and friction force to the main cutting force also decrease with increasing material removal temperature during LAM of PSZ^[53], which suggests a reduction in the friction coefficient at high material

removal temperatures.

4.3 Tool Materials and Wear

Polycrystalline diamond (PCD) tool is not suitable for LAM because of its low carburizing temperature ($900 \text{ }^\circ\text{C}$)^[53]. Polycrystalline cubic boron nitride (PCBN) has been used for LAM of Si_3N_4 ^[52,59] and PSZ^[53], and carbide insert has been used for LAM of mullite^[54] and Al_2O_3 ^[63] ceramics. PCBN tool shows significantly longer tool life than tungsten carbide tool when LAM of PSZ at the same cutting conditions^[53]. But Klocke *et al.*^[62] showed that flank wear was smaller by using PCD tool than that by using CBN tool during LAM of Si_3N_4 .

Flank wear is found to be the dominant tool failure mode during laser assisted turning of ceramics as shown in Fig. 12. The tool life is much longer during LAM than that in the conventional machining of mullite^[54]. The flank wear is attributed to the adhesion of the glassy grain-boundary phase to the cutting tool. The bonding between the glassy phase and cutting tool may be broken during machining and this can result in tearing of the cutting tool material^[52,53].

Repeatingly, tool wear is strongly dependent on the material removal temperature, and there is an optimum material removal temperature for longer tool life. A short tool life below or above the optimum material removal temperature is due to an insufficient reduction in workpiece strength and reduction of tool strength by overheating, respectively^[54]. Therefore, tool life can be optimized by maintaining the material removal temperature in the optimum region.

The tool failure mode for laser assisted milling

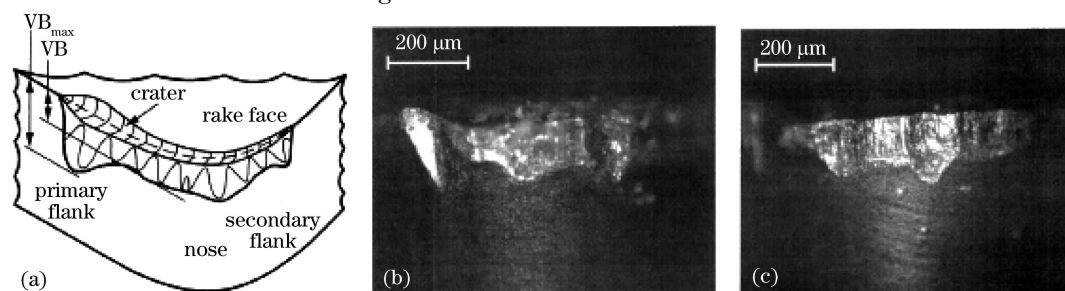


Fig. 12 (a) Schematic of tool wear; (b) flank face; (c) nose during LAM of PSZ^[53]

of Si_3N_4 is edge chipping at workpiece temperature lower than the softening point of glass phase due to the high and frequent dynamic impact on the cutting edge when the tool is engaged with workpiece during cutting. Gradual flank wear is the dominant tool failure mode at high workpiece temperature and the flank wear is significantly reduced with increasing workpiece temperature up to a point, further increase in temperature has less or negative influence on reduction in tool wear^[27,30]. The maximum workpiece temperature allowed for reducing tool wear in laser assisted milling is higher than that in laser assisted turning because of the lower temperature of insert as a result of shorter tool – chip contact time in milling operation^[27].

4.4 Surface Integrity

The integrity of the machined surface is assessed by measuring surface roughness and observing surface or subsurface damage. Above a certain temperature, the machined surface after LAM of Si_3N_4 is characterized by the build-up of irregular glassy phase debris and the formation of cavities due to $\beta\text{-Si}_3\text{N}_4$ grain pullout^[52,59]. Similar to LAM of PSZ^[53], the surface roughness is not sensitive to the material removal temperature, but depends on the size and distribution of Si_3N_4 grains.

Local cracks presented in the HAZ without cutting indicate that the laser heating cycle introduces high thermal stress in PSZ^[53]. The thickness of the cracking region increases with the material removal temperature (laser power). If this thickness is greater than the depth of cut, the crack may remain in the subsurface, which is detrimental for the properties of the machined part. Therefore, the material removal temperature must be controlled to produce a damage-free component by LAM.

The sudden impact and stress release between cutting tool and workpiece when the cutting tool enters and leaves the workpiece during milling of ceramics (Si_3N_4) result in workpiece edge chipping at both the entry and exit edges. The workpiece edge chipping leads to poor dimensional and geometric accuracy and is the source of cracking. Although the workpiece edge chipping can not be avoided completely, it can be reduced significantly due to the increasing workpiece temperature during laser assisted milling. Reduction of workpiece edge chipping is the coupling effects of softening and toughening mechanisms, the latter only takes positive

effect when temperature is above brittle/ductile transition temperature and below the global softening temperature (between 1200 and 1400 °C)^[64].

Compressive residual stress is observed on the laser assisted machined surface of Si_3N_4 in both axial and hoop directions^[45]. However its magnitude is smaller than that produced by conventional grinding^[45,62] because the softening of glassy phase can significantly relieve the stress at the material removal zone^[45]. Klocke *et al.*^[62] reported that the bending strength and the Weibull modulus of Si_3N_4 components made by LAM were better than those by grinding.

4.5 Optimization and Energy Efficiency of LAM of Ceramics

Optimum range of the material removal temperature is determined by comparing the specific cutting energy (u_c), tool life, scrap rate (determined by the damage on the machined surface in the form of cracks and spalling), and surface roughness as shown in Fig. 13. The optimum material removal temperature is in a range from approximately 900 to 1100 °C for PSZ^[53].

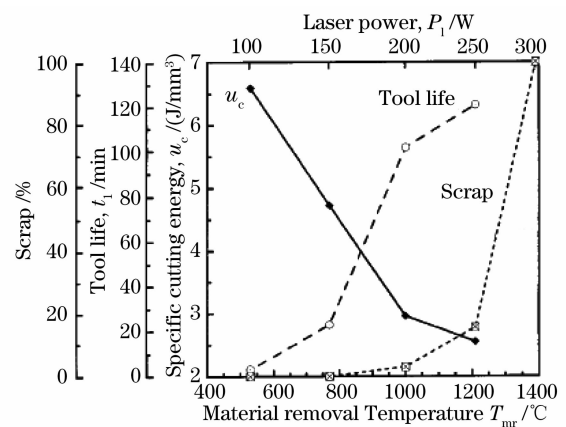


Fig. 13 Effect of material removal temperature on specific cutting energy, tool life, and scrap rate for PSZ^[53]

During LAM process, the energy absorbed by the workpiece not only raises the temperature of the material to be removed to the desired material removal temperature, but also heats the material near the removal zone. A preheating efficiency is defined as the ratio of the minimum power to heat the material to be removed to the desired material removal temperature to the total amount of energy absorbed from the external heat source^[65]. This efficiency decreases with increasing material removal temperature because large amount of energy is wasted to heat materials outside the cutting zone. As a metric, the preheating efficiency can be used to

guide the configuration of laser beam, such as its focusing location and position with cutting tool in consideration of workpiece material's thermo-physical properties.

5 Conclusion

LAM uses a laser beam as an external heat source to heat and soften the workpiece and facilitates the machining of ceramics with conventional cutting tool. Generally, it offers lower cutting forces, longer tool life, and better machining surface. The local temperature of material as it enters the shear deformation zone plays an important role in LAM process. It has to be maintained in the optimum range to achieve the maximum benefit of LAM. The integration of a laser beam with machining tool in milling operation is still a challenge. A motor independent of the machining spindle is required to move the laser beam to travel the same path as the cutting tool.

LAM is a complicated process, the laser beam not only changes the flow stress, but also changes the deformation behaviour of workpiece and friction between chip and tool. So far, intensive experimental works and modelling on temperature distribution have been reported. Investigation into the deformation behaviour of workpiece materials under high temperature and high strain rate, friction between cutting tool and workpiece materials at high temperature and chip separation are required to fully understand the LAM process.

References

- 1 W. König, A. K. Zaboklicki. Laser-assisted hot machining of ceramics and composite materials [C]. *International Conference on Machining of Advanced Materials*, 1994, **847**:455~463
- 2 J. W. Novak, Y. C. Shin, F. P. Incropera. Assessment of plasma enhanced machining for improved machinability of Inconel 718 [J]. *J. Manufacturing Science and Engineering, Transactions of the ASME*, 1997, **119**:125~129
- 3 C. E. Leshock, J.-N. Kim, Y. C. Shin. Plasma enhanced machining of inconel 718: modeling of workpiece temperature with plasma heating and experimental results [J]. *International J. Machine Tools & Manufacture*, 2001, **41**:877~897
- 4 L. N. L. D. Lacalle, J. A. Sánchez, A. Lamikiz *et al.*. Plasma assisted milling heat-resistant superalloys [J]. *J. Manufacturing Science and Engineering, Transactions of the ASME*, 2004, **126**:274~285
- 5 J. H. Lemelson. Machining method and apparatus [P]. US Patent: 4,733,049
- 6 L. Özler, A. İnan, C. Özel. Theoretical and experimental determination of tool life in hot machining of austenitic manganese steel [J]. *International J. Machine Tools & Manufacture*, 2001, **41**:163~172
- 7 K. P. Maitya, P. K. Swain. An experimental investigation of hot-machining to predict tool life [J]. *J. Materials Processing Technology*, 2008, **198**:344~349
- 8 N. Tosun, L. Özler. A study of tool life in hot machining using artificial neural networks and regression analysis method [J]. *J. Materials Processing Technology*, 2002, **124**:99~104
- 9 M. A. Lajis, A. K. M. N. Amin, A. N. M. Karim *et al.*. Hot machining of hardened steels with coated carbide inserts [J]. *American J. Engineering and Applied Sciences*, 2009, **2**:421~427
- 10 G. Chryssolouries, N. Anifantis, S. Karagiannis. Laser assisted machining: An overview [J]. *Journal of Manufacturing Science & Engineering, Transactions of the ASME*, 1997, **119**:766~769
- 11 J. C. Rozzi, F. E. Pfefferkorn, F. P. Incropera *et al.*. Transient thermal response of rotating cylindrical silicon nitride workpiece subjected to translating laser heat source, Part I: Comparison of surface temperature measurements with theoretical results [J]. *J. Heat Transfer*, 1998, **120**:899~906
- 12 F. E. Pfefferkorn, F. P. Incropera, Y. C. Shin. Heat transfer model of semi-transparent ceramics undergoing laser-assisted machining [J]. *International J. Heat and Mass Transfer*, 2005, **48**:1999~2012
- 13 X. Wu, H. Zhang, Y. Wang. Three-dimensional thermal analysis for Laser assisted machining of ceramics using FEA [C]. *SPIE*, 2009, **7282**:72822I
- 14 P. Dumitrescu, P. Koshy, J. Stenekes *et al.*. High-power diode laser assisted hard turning AISI D2 tool steel [J]. *International J. Machine Tools & Manufacture*, 2006, **46**:2009~2016
- 15 J.-F. Wu, Y.-B. Guu. Laser assisted machining methods and device [P]. US Patent: 7002100 B2
- 16 M. C. Longo. Working piece by laser beam [P]. US Patent: 4,229,640
- 17 S. Sun, J. Harris, M. Brandt. Parametric investigation of laser-assisted machining of commercially pure titanium [J]. *Advanced Engineering Materials*, 2008, **10**:565~572
- 18 S. Rajagopal, D. J. Plankenhorn, V. L. Hil. Machining aerospace alloys with the aid of a 15 kW laser [J]. *J. Applied Metalworking*, 1982, **2**:170~184
- 19 M. Weck, W. V. Zeppelin, C. Hermanns. Laser-a tool for turning centres [C]. in: F. V. M. Geiger (Ed.) *Laser Assisted Net Shape Engineering, Proceedings of the LANE'94, Vol 1, Meisenbach Bamberg*, 1994. 427~437
- 20 J. F. Gratiás, L. J. Fan, G. Marot *et al.*. Proposition of a method to optimize the machining of XC42 steel with laser assistance [J]. *CIRP Annals*, 1993, **42**:115~118
- 21 W. B. Salem, G. Marot, A. Moisan *et al.*. Laser assisted turning during finishing operation applied to hardened steels and Inconel 718 [C]. in: F. V. M. Geiger (Ed.) *Laser Assisted Net Shape Engineering, Proceedings of the LANE'94, Vol 1, Meisenbach Bamberg*, 1994. 455~464
- 22 Y. C. Shin. Laser assisted machining process with distributed lasers [P]. US Patent: 0062920 A1
- 23 M. Anderson, Y. C. Shin. Laser-assisted machining of an austenitic stainless steel: P550 [C]. *Proc. IMechE, Part B: J. Engineering Manufacture*, 2006, **220**:2055~2067
- 24 M. Anderson, R. Patwa, Y. C. Shin. Laser-assisted machining of Inconel 718 with an economic analysis [J]. *International J. Machine Tools & Manufacture*, 2006, **46**:1879~1891
- 25 K. Armitage. Laser assisted machining of high chromium white cast iron [D]. Master's thesis, Swinburne University of Technology, 2005
- 26 J. Walter, R. Ritzi. Increasing tool life by laser assisted turning [C]. in: A. O. M. Geiger (Ed.) *Laser Assisted Net Shape Engineering 4, Proceedings of the LANE 2004, Vol 2, Meisenbach Bamberg*, 2004. 1157~1164
- 27 B. Yang, S. Lei. Laser-assisted milling of silicon nitride ceramic: a machinability study [J]. *International J. Mechatronics and Manufacturing Systems*, 2008, **1**:116~130
- 28 T. Thomas, J. O. Vigneau. Laser-assisted milling process [P]. US Patent: 5906459
- 29 A. Demmer, S. Bausch, K. Groll. Perspectives for laser-assisted

- machining: Cost-effective processing of difficult-to machine materials. The industrial laser user, 2005. 38~41
- 30 Y. Tian, B. Wu, M. Anderson *et al.*. Laser-assisted milling of silicon nitride and Inconel 718 [J]. *J. Manufacturing Science and Engineering*, 2008, **130**:031013-031011-031013-031019
- 31 H. Hügel, M. Wiedmaier, T. Rudlaff. Laser processing integrated into machine tool-design, applications, economy [C]. in: F. V. M. Geiger (Ed.) Laser Assisted Net Shape Engineering, Proceedings of the LANE94, Vol 1, Meisenbach Bamberg, 1994. 439~453
- 32 H. Hügel, M. Wiedmaier, T. Rudlaff. Laser processing integrated into machine tool-design, applications, economy [J]. *Optical and Quantum Electronics*, 1995, **27**:1149~1164
- 33 C.-W. Chang, C.-P. Kuo. An investigation of laser-assisted machining of Al₂O₃ ceramics planing [J]. *International Journal of Machine Tools & Manufacture*, 2007, **47**:452~461
- 34 Y. Tian, Y. C. Shin. Laser-assisted burnishing of metals [J]. *International J. Machine Tools & Manufacture*, 2007, **47**:14~22
- 35 Y. Tian, Y. C. Shin. Thermal modelling and experimental evaluation of laser-assisted dressing of superabrasive grinding wheels [C]. *Proc. IMechE, Part B: J. Engineering Manufacture*, 2007, **221**:605~616
- 36 C. Zhang, Y. C. Shin. A novel laser-assisted truing and dressing technique for vitrified CBN wheels [J]. *International J. Machine Tools & Manufacture*, 2002, **42**:825~835
- 37 C. Zhang, Y. C. Shin. Wear of diamond dresser in laser assisted truing and dressing of vitrified CBN wheels [J]. *International J. Machine Tools & Manufacture*, 2003, **43**:41~49
- 38 E. Westkämper. Grinding assisted by Nd-YAG lasers [J]. *CIRP Annals*, 1995, **44**:317~320
- 39 Q. M. Murphy. Apparatus and process for laser assisted drilling [P]. US Patent, 5409376
- 40 P. A. Rebroy, F. E. Pfefferkorn, Y. C. Shin *et al.*. Comparative assessment of laser-assisted machining for various ceramics [J]. *Transactions of North American Manufacturing Research Institution*, 30, **2002**:153~160
- 41 M. Ignatiev, L. Okorokov, I. Smurov *et al.*. Laser assisted machining: process control based on real-time surface temperature measurements [J]. *J. De Physique*, 1994, **4**:C4-65-C64-68
- 42 F. E. Pfefferkorn, J. C. Rozzi, F. P. Incropera *et al.*. Surface temperature measurement in laser-assisted machining processes [J]. *Experimental Heat Transfer*, 1997, **10**:291~313
- 43 F. E. Pfefferkorn, F. P. Incropera, Y. C. Shin. Surface temperature measurement of semi-transparent ceramics by long-wavelength pyrometry [J]. *Transactions ASME, J. Heat Transfer*, 2003, **125**:48~56
- 44 P. A. Rebroy, Y. C. Shin, F. P. Incropera. Design of operating conditions for crackfree laser-assisted machining of mullite [J]. *International J. Machine Tools and Manufacture*, 2004, **44**:677~694
- 45 Y. Tian, Y. C. Shin. Laser-assisted machining of damage-free silicon nitride parts with complex geometric features via in-process control of laser power [J]. *J. Am. Ceram. Soc.*, 2006, **89**:3397~3405
- 46 S. Skvarenina, Y. C. Shin. Laser-assisted machining of compacted graphite iron [J]. *International J. Machine Tools & Manufacture*, 2006, **46**:7~17
- 47 Y. Tian, Y. C. Shin. Thermal modeling for laser-assisted machining of silicon nitride ceramics with complex features [J]. *J. Manufacturing Science and Engineering, Transactions of the ASME*, 2006, **128**:425~434
- 48 J. C. Rozzi, F. P. Incropera, Y. C. Shin. Transient thermal response of rotating cylindrical silicon nitride workpiece subjected to translating laser heat source, Part II : parametric effects and assessment of a simplified model [J]. *J. Heat Transfer*, 1998, **120**:907~915
- 49 J. C. Rozzi, F. E. Pfefferkorn, F. P. Incropera *et al.*. Transient, three-dimensional heat transfer model for the laser assisted machining of silicon nitride: I-comparison of predictions with measured surface temperature histories [J]. *International J. Heat and Mass Transfer*, 2000, **43**:1409~1424
- 50 J. C. Rozzi, F. P. Incropera, Y. C. Shin. Transient, three-dimensional heat transfer model for the laser assisted machining of silicon nitride: II-assessment of parametric effects [J]. *International J. Heat and Mass Transfer*, 2000, **43**:1425~1437
- 51 N. Yang, M. Brandt, S. Sun. Numerical and experimental investigation of the heat-affected zone in a laser assisted machining of Ti6Al4V alloy process [J]. *Materials Science Forum*, 2009, **618-619**:143~146
- 52 S. Lei, Y. C. Shin, F. P. Incropera. Experimental investigation of thermo-mechanical characteristics in laser assisted machining of silicon nitride ceramics [J]. *J. Manufacturing Science and Engineering, Transactions of the ASME*, 2001, **123**:639~646
- 53 F. E. Pfefferkorn, Y. C. Shin, F. P. Incropera *et al.*. Laser-assisted machining of magnesia-partially-stabilized zirconia [J]. *Transactions ASME, J. Manufacturing Science and Engineering*, 2004, **126**:42~51
- 54 P. A. Rebroy, Y. C. Shin, F. P. Incropera. Laser-assisted machining of reaction sintered mullite ceramics [J]. *J. Manufacturing Science and Engineering, Transactions of the ASME*, 2002, **124**:875~885
- 55 R. Singh, M. J. Alberts, S. N. Melkote. Characterization and prediction of the heat-affected zone in a laser-assisted mechanical micromachining process [J]. *International J. Machine Tools & Manufacture*, 2008, **48**:994~1004
- 56 G. Germain, F. Morel, J.-L. Lebrun *et al.*. Machinability and surface integrity for a bearing steel and a titanium alloy in laser assisted machining (optimisation on LAM on two materials) [J]. *Lasers in Engineering*, 2007, **17**:329~344
- 57 A. N. Samant, N. B. Dahotre. Laser machining of structural ceramics—A review [J]. *J. the European Ceramic Society*, 2009, **29**:969~993
- 58 S. Lei, Y. C. Shin, F. P. Incropera. Deformation mechanisms and constitutive modeling for silicon nitride undergoing laser assisted machining [J]. *International J. Machine Tools & Manufacture*, 2000, **40**:2213~2233
- 59 J. C. Rozzi, F. E. Pfefferkorn, Y. C. Shin *et al.*. Experimental evaluation of the laser assisted machining of silicon nitride ceramics [J]. *J. Manufacturing Science and Engineering, Transactions of the ASME*, 2000, **122**:666~670
- 60 Y. Tian, Y. C. Shin. Multiscale finite element modeling of silicon nitride ceramics undergoing laser-assisted machining [J]. *ASME Transactions, J. Manufacturing Science and Engineering*, 2007, **129**:287~295
- 61 K. J. Bowman, F. E. Pfefferkorn, Y. C. Shin. Recrystallization textures during laser-assisted machining of zirconia ceramics [J]. *Materials Science Forum*, 2002, **408-412**:1669~1674
- 62 F. Klocke, T. Bergs. Laser-assisted turning of advanced ceramics [C]. *SPIE*, 1997, **3102**:120~130
- 63 C. Chang, C. Kuo. Evaluation of surface roughness in LAM of aluminum oxide ceramics with Taguchi method [J]. *International J. Machine Tools and Manufacturing*, 2007, **47**:141~147
- 64 B. Yang, X. Shen, S. Lei. Mechanisms of edge chipping in laser-assisted milling of silicon nitride ceramics [J]. *International J. Machine Tools & Manufacture*, 2009, **49**:344~350
- 65 F. E. Pfefferkorn, S. Lei, Y. Jeon *et al.*. A metric for defining the energy efficiency of thermally assisted machining [J]. *International Journal of Machine Tools & Manufacture*, 2009, **49**:357~365